Non-Abelian Energy Loss at Finite Opacity

M. Gyulassy,[1] P. Levai,[1,2] and I. Vitev[1]

[1]*Department of Physics, Columbia University, 538 West 120th Street, New York, New York 10027*
[2]*KFKI Research Institute for Particle and Nuclear Physics, P.O. Box 49, Budapest, 1525, Hungary*
(Received 12 May 2000)

A systematic expansion in opacity, L/λ, is used to clarify the nonlinear behavior of induced gluon radiation in quark-gluon plasmas. The inclusive differential gluon distribution is calculated up to second order in opacity and compared to the zeroth order (factorization) limit. The opacity expansion makes it possible to take finite kinematic constraints into account that suppress jet quenching in nuclear collisions below RHIC ($\sqrt{s} = 200$ AGeV) energies.

Introduction.—The production of high transverse momentum jets in quantum chromodynamics processes is always accompanied by gluon showers. For jets produced inside nuclei final state interactions of jet and radiated gluons induce further radiation and also broaden the gluon shower. The non-Abelian radiative energy loss in a medium is expected to be observable as "jet quenching." The detectable consequences in nuclear collisions should be seen as a suppression of the high $p_\perp$ tails of single hadron distributions [1,2] and a broadening of the jet cone [3].

Non-Abelian energy loss in perturbative quantum chromodynamics can be calculated analytically in two limits. In both cases, the energy of the leading parton is assumed to be large enough that its angular deflection can be neglected. One analytic limit applies to thin plasmas where the mean number, $\bar{n} = L/\lambda$, of jet scatterings is small [4,5]. The other limit is the thick plasma one [6–9], where $\bar{n} \gg 1$. This mean number, $\bar{n}$, is a measure of the opacity or geometrical thickness of the medium:

$$\bar{n} = \frac{N\sigma_{\text{el}}}{A_\perp} = \int dz(\sigma_{\text{el}}\rho) \approx \frac{dN}{dy} \frac{\sigma_{\text{el}}}{2\pi R_G^2} \log \frac{R_G}{\tau_0}. \quad (1)$$

For a constant (box) density $\rho = N/LA_\perp$, L is the target thickness and $\lambda = 1/\sigma_{\text{el}}\rho$ is the average mean free path. For a sharp cylinder geometry we can interpret $L = 1.2A^{1/3} \equiv R_s$ as the nuclear radius. For a more realistic 3 + 1D expanding Gaussian cylinder with $\rho(\mathbf{x}_\perp, \tau) = (\tau_0/\tau)\rho_0 \exp[-(\mathbf{x}_\perp^2 + \Delta\tau^2)/R_G^2]I_0(2|\mathbf{x}_\perp|\Delta\tau/R_G^2)$, L is replaced by the equivalent rms Gaussian transverse radius $R_G = 0.75A^{1/3}$ fm. The rightmost form in (1) is obtained by averaging over the expanding Gaussian cylinder. Here τ_0 is the formation time of the plasma and $\rho_0 = \rho(\mathbf{0}_\perp, \tau_0)$ is the initial central density.

At relativistic heavy ion collider (RHIC) energies ($\sqrt{s} \sim 200$ AGeV) the expected rapidity density of the gluons is $dN/dy \sim 1000$ for $A = 200$. With an elastic cross section $\sigma_{\text{el}} \sim 2$ mb and a plasma formation time ~ 0.5 fm/c, we obtain $\bar{n} \sim 4$. This suggests that neither analytic approach may be strictly applicable in practice. However, because

of the non-Abelian analog [4,6,8] of the Landau-Pomeranchuk-Migdal (LPM) effect, the radiation intensity angular distribution and total energy loss are controlled by the combined effect of the number of scatterings $\bar{n} = L/\lambda$ and a formation probability $p_f = L/l_f = L\mu^2/2xE$ of the gluon in the medium. In [6,8] the induced energy loss was shown to be nonlinear in the nuclear thickness, $\Delta E \propto \mu^2 L^2/\lambda$ assuming the $\bar{n} \gg 1$ limit. In [5], we showed that the angular pattern was even more strongly nonlinear in the exclusive (tagged target) case. We show below that, in the inclusive case in the small x limit, important features of the radiation pattern are in fact governed by the product $\bar{n}p_f = L^2\mu^2/2xE\lambda$. Because of this, even the first order in opacity reproduces the L^2 dependence of the energy loss and the range of applicability of the finite opacity expansion derived below may extend to realistic targets. The modifications to the results in the $x \to 1$ regime are also discussed below based on Ref. [7].

Another important motivation for our approach is the apparent absence of jet quenching observed at SPS energies [10,11]. As we find below, the opacity expansion shows that finite kinematic constraints suppress greatly the non-Abelian energy loss at SPS energies. The work reported in this Letter extends Ref. [5] by including virtual corrections [7] necessary to compute inclusive (vs tagged) jet quenching. This provides a natural unitarizing procedure with detailed derivation of the results given in Ref. [12].

Hard gluon distribution.—At zeroth order in opacity, the gluon emission from the hard production vertex with momenta of jet and gluon in light-cone coordinates [5,12] $p = [(1 - x)E^+, p^-, \mathbf{p}_\perp], k = [xE^+, k^-, \mathbf{k}_\perp]$ is given in the leading pole approximation (LPA) by

$$x\frac{dN^{(0)}}{dx\,d\mathbf{k}_\perp^2} = \frac{C_R\alpha_s}{\pi}\left(1 - x + \frac{x^2}{2}\right)\frac{1}{\mathbf{k}_\perp^2}, \quad (2)$$

where $x = k^+/E^+ \approx \omega/E$, and C_R is the Casimir of the (spin 1/2) jet in the d_R dimensional color representation. For a spin 1 jet the gluon splitting function must be substituted above. The differential energy distribution outside a cone defined by $\mathbf{k}_\perp^2 > \mu^2$ is given by

$$\frac{dI^{(0)}}{dx} = \frac{2C_R\alpha_s}{\pi}\left(1 - x + \frac{x^2}{2}\right)E\log\frac{|\mathbf{k}_\perp|_{max}}{\mu}, \quad (3)$$

where the upper kinematic limit is

$$\mathbf{k}_{\perp\,max}^2 = \min[4E^2x^2, 4E^2x(1-x)]. \quad (4)$$

The energy loss outside the cone is then given by

$$\Delta E^{(0)} = \frac{4C_R\alpha_s}{3\pi}E\log\frac{E}{\mu} \quad (5)$$

in the leading $\log(E/\mu)$ approximation. While this overestimates the radiative energy loss in the vacuum (self-quenching), it is important to note that $\Delta E^{(0)}/E \sim 50\%$ is typically much larger than the medium induced energy loss.

Opacity expansion.— To compute the induced radiation, we assume as in [4,5] that the quark gluon plasma can be modeled by N well-separated, i.e., $\lambda \gg 1/\mu$, color-screened Yukawa potentials. In contrast to [5], we consider here the *inclusive* gluon distribution induced by a finite medium which remains *unobserved*. Without target tagging, we must add double Born (virtual) amplitudes [12] to the real (direct) amplitudes derived in [5]. We denote by G_0 the basic eikonal hard emission amplitude in the $x \ll 1$ regime

$$G_0 = -2ig_s\boldsymbol{\epsilon}_\perp \cdot \mathbf{H}e^{i\omega_0 z_0}c, \quad (6)$$

where we use the shorthand notation of [5], $\mathbf{H} \equiv \mathbf{k}_\perp/\mathbf{k}_\perp^2$, $\omega_0 \equiv \mathbf{k}_\perp^2/2xE$. The hard parton originates at z_0, and c denotes the color matrix T_c in its d_R dimensional representation. In Ref. [12] we developed an iterative procedure to generate from this amplitude the sum of all amplitudes in the small x limit to *any* order in opacity including both direct and virtual terms.

To first order in opacity cross section for the induced radiation consists of 3^2 real and 2×4 double Born contributions that sum to a simple result

$$P^{(1)} \propto C_R C_A d_R\{(-2\mathbf{C}_1 \cdot \mathbf{B}_1)[1 - \cos(\omega_1\Delta z_1)]\}, \quad (7)$$

where $\mathbf{C}_m$ and ω_m are obtained from $\mathbf{H}$ and ω_0 through the substitution $\mathbf{k}_\perp \Rightarrow \mathbf{k}_\perp - \mathbf{q}_{\perp m}$. Here $\mathbf{q}_{\perp m}$ is the momentum transfer at location z_m. The shorthand $\mathbf{B}_m \equiv \mathbf{H} - \mathbf{C}_m$ and $\Delta z_m \equiv z_m - z_{m-1}$ [5,12]. Note that the interaction of the radiated gluon in the medium brings in a factor $C_A = N_c$. Unlike the tagged case [5], the above first order correction to the hard (factorization) distribution in Eq. (2) has no simple classical cascade interpretation. In the tagged case, the result contained terms with color factors $C_R^2 d_R$ as well as $C_R C_A d_R$ that were easily interpretable in terms of jet rescattering and induced radiation. In the inclusive case, the unitarity corrections lead to long range nonlocal color interference effects that result in a remarkable "color triviality" property [13]. In fact all jet rescattering effects cancel [6,7]. As derived in Ref. [12], the color factor at order n is simply $C_R C_A^n d_R$, in contrast to the vastly more complicated color structure of the tagged case [5].

The non-Abelian LPM effect is seen in Eq. (7) as arising from the gluon formation factor

$$\Phi(\Delta z_1) = 1 - \cos(\omega_1\Delta z_1). \quad (8)$$

This must also be averaged over the longitudinal target profile, $n(z)$. For a box density [6] of thickness $L = 1.2A^{1/3}$, $n = \theta(L - z)/L$. For analytic simplicity we take instead an exponential form $n_e(z) = e^{-z/L_e}/L_e$. In order to compare results for the two cases, we must require identical mean target depths, i.e., $L_e = L/2$. With $n_e(z)$ the ensemble averaged formation factor is

$$\int_0^\infty \frac{2d\Delta z_1}{L}e^{-(2\Delta z_1/L)}\Phi(\Delta z_1) = \frac{(\mathbf{k} - \mathbf{q}_1)_\perp^4 L^2}{16x^2E^2 + (\mathbf{k} - \mathbf{q}_1)_\perp^4 L^2}. \quad (9)$$

The formation probability in this case is controlled by simple Lorentzian factors. [Note that for $x \rightarrow 1$ one should include above a modification of the energy difference, ω_1, that leads to $x \rightarrow x(1 - x)$ [7].]

Averaging over the momentum transfer $\mathbf{q}_{1\perp}$ via the color Yukawa potential leads finally to the $x \ll 1$ gluon double differential distribution

$$x\frac{dN^{(1)}}{dx\,d\mathbf{k}_\perp^2} = x\frac{dN^{(0)}}{dx\,d\mathbf{k}_\perp^2}\frac{L}{\lambda_g}\int_0^{q_{max}^2}d^2\mathbf{q}_{1\perp}\frac{\mu_{eff}^2}{\pi(\mathbf{q}_{1\perp}^2 + \mu^2)^2}$$
$$\times \frac{2\mathbf{k}_\perp \cdot \mathbf{q}_{1\perp}(\mathbf{k} - \mathbf{q}_1)_\perp^2 L^2}{16x^2E^2 + (\mathbf{k} - \mathbf{q}_1)_\perp^4 L^2}. \quad (10)$$

where the opacity factor $L/\lambda_g = N\sigma_{el}^{(g)}/A_\perp$ arises from the sum over the N distinct targets. Note that the radiated gluon mean free path $\lambda_g = (C_A/C_R)\lambda$ appears rather than the jet mean free path. It is the color triviality of Eq. (7) that allows us to absorb C_R factor into the hard distribution, Eq. (2), and C_A factor into λ_g.

The upper kinematic bound on the momentum transfer $q_{max}^2 = s/4 \simeq 3E\mu$, $[1/\mu_{eff}^2 = 1/\mu^2 - 1/(\mu^2 + q_{max}^2)]$. For SPS and RHIC energies, this finite limit cannot be ignored as we show below.

The second order contribution in opacity requires a more complex calculation involving the sum of 7^2 direct and 2×86 virtual terms as discussed in [12]

$$P^{(2)} \propto C_R C_A^2 d_R\{2\mathbf{C}_1 \cdot \mathbf{B}_1[1 - \cos(\omega_1\Delta z_1)] + 2\mathbf{C}_2 \cdot \mathbf{B}_2\{\cos(\omega_2\Delta z_2) - \cos[\omega_2(\Delta z_1 + \Delta z_2)]$$
$$- 2\mathbf{C}_{(12)} \cdot \mathbf{B}_2[\cos(\omega_2\Delta z_2) - \cos(\omega_{(12)}\Delta z_1 + \omega_2\Delta z_2)] - 2\mathbf{C}_{(12)} \cdot \mathbf{B}_{2(12)}[1 - \cos(\omega_{(12)}\Delta z_1)]\}, \quad (11)$$

where with $\mathbf{C}_{(mn)}$ and $\omega_{(mn)}$ obtained from $\mathbf{H}$ and ω_0 through the substitution $\mathbf{k}_\perp \Rightarrow \mathbf{k}_\perp - \mathbf{q}_{\perp m} - \mathbf{q}_{\perp n}$ and $\mathbf{B}_{m(nl)} \equiv \mathbf{C}_m - \mathbf{C}_{(nl)}$ [5,12]. Both probabilities Eqs. (7) and (11), actually hold for either quark or gluon jets in the small x approximation.

The general closed form expression for $P^{(n)}$ for arbitrary n is derived in Ref. [12]. We note that in the two important limits $|\mathbf{k}_\perp| \to 0$ and $|\mathbf{k}_\perp| \to \infty$ the induced radiation at any order is negligible relative to $dN^{(0)}$ for any fixed x due to the singular $\mathbf{k}_\perp$ dependence of $dN^{(0)}$ and azimuthal angular averaging. This is clearly seen in Fig. 1 up to second order.

The average over the scattering points, z_1, z_2 in the second order case is performed with the exponential density profile as follows:

$$\langle \cdots \rangle = \int_0^\infty \frac{3 d\Delta z_1}{L} \int_0^\infty \frac{3 d\Delta z_2}{L} e^{-\frac{3(\Delta z_1 + \Delta z_2)}{L}} \cdots . \quad (12)$$

We must use $L_e = L/(n + 1)$ for nth order in opacity in order to ensure that the first moment of the mth scattering center is identical to that in a box distribution $[\langle z_m \rangle_n = mL/(n + 1)]$ as discussed in [5].

Numerical results comparing the first and second order in opacity corrections to the hard distribution Eq. (2) are illustrated in Figs. 1 and 2.

We consider a 50 GeV quark jet in a medium with $\lambda_g = 1$ fm. A screening scale $\mu = 0.5$ GeV and $\alpha_s = 0.3$ were assumed. The "angular" distribution in Fig. 1 shows that the first order angular distribution is wider than the medium independent hard $1/\mathbf{k}_\perp^2$ distribution. The second order corrections redistribute the gluons further. In Fig. 2 the $\mathbf{k}_\perp$ integrated contributions to the gluon intensity, dI/dx, are shown for the same conditions as in Fig. 1 extrapolated to $x \sim 0.5$. Note that for $x > 0.5$ the $1/(1 - x)$ dependence leads to additional contributions from the $x \to 1$ region [see Eq. (15) and also [7]]. The induced intensity is concentrated at small x in contrast to the relatively constant intensity originating from the hard "self-quenching" term (3). The long $1/x$ tail contributes, however, a logarithmic factor $\log(E/\mu)$ as we discuss further below. The second

order correction suppresses the intensity at small x and enhances it somewhat at higher $x \gtrsim 0.2$. We note that these two effects tend to cancel in the integrated energy loss as seen in Fig. 3.

Radiation intensity and energy loss.—To gain analytic insight into the above numerical results, we consider the first order induced radiation intensity $dI^{(1)}/dx$ in the approximation that $\mathbf{k}_{\perp \max}^2 = \infty$. This allows us to change variables $\mathbf{q}'_\perp \equiv \mathbf{k}_\perp - \mathbf{q}_{1\perp}$ in Eq. (10) and express the integrand in the azimuthal ϕ integral as a partial derivative with respect to $\mathbf{k}_\perp^2$. The remaining $\mathbf{q}'^2_\perp/\mu^2$ integral (cutoff at $1/\delta < \infty$) can be performed then analytically, resulting in

$$\frac{dI^{(1)}}{dx} = \frac{C_R \alpha_s}{\pi} \left(1 - x + \frac{x^2}{2} \right) E \frac{L}{\lambda_g} f(\gamma, \delta), \quad (13)$$

where $\gamma = L\mu^2/4x(1 - x)E$ is the effective formation probability including the $(1 - x)$ modification expected in the $x \to 1$ limit [7]. The formation function in this approximation is given by

$$f(\gamma, \delta) = \frac{\gamma(2 \tan^{-1} \frac{\gamma}{\delta} + \gamma \log \frac{\gamma^2 + \delta^2}{(1 + \delta)^2})}{(1 + \gamma^2)}, \quad (14)$$

which in the $\delta \to 0$ and $\gamma \ll 1$ limit reduces to a simple form $f(\gamma, 0) \approx \pi\gamma \propto L$. This special limit leads to a quadratic dependence on L:

$$\frac{dI^{(1)}}{dx} \approx \frac{C_R \alpha_s}{4} \frac{1 - x + \frac{x^2}{2}}{x(1 - x)} \frac{L^2 \mu^2}{\lambda_g}. \quad (15)$$

This formula breaks down at both $x \to 0$ and $x \to 1$ because $|\mathbf{k}_\perp|_{\max}$ cannot be approximated by ∞.

The total radiative energy loss is then given by

$$\Delta E^{(1)} = \frac{C_R \alpha_s}{N(E)} \frac{L^2 \mu^2}{\lambda_g} \log \frac{E}{\mu}, \quad (16)$$

with $N(\infty) = 4$ if the kinematic bounds are ignored as in Eq. (15). In practice, we emphasize that finite kinematic constraints cause $N(E)$ to deviate considerably from the asymptotic value 4. We find that $N(E) = 7.3$, 10.1, 24.4 for $E = 500$, 50, 5 GeV if the $(1 - x)$ factor is neglected. The large x contributions typically decrease $N(E)$
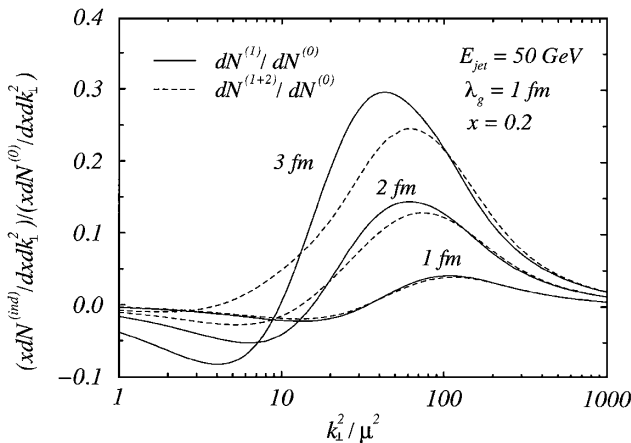

FIG. 1. The medium induced gluon differential multiplicity normalized by the factorization distribution Eq. (2) is plotted vs $\mathbf{k}_\perp^2/\mu^2$ for opacity $L/\lambda_g = 1, 2, 3$. Solid curves show first order (10) and dashed including second order in opacity (11) for a gluon with $x = 0.2$. (Quark jet of $E_{\text{jet}} = 50$ GeV and $\mu = 0.5$ GeV.)
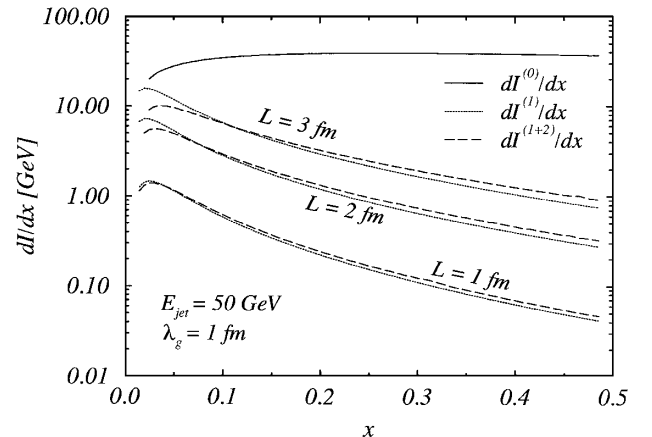

FIG. 2. The contributions to the induced radiation intensity to first and second order in opacity are compared to Eq. (3).
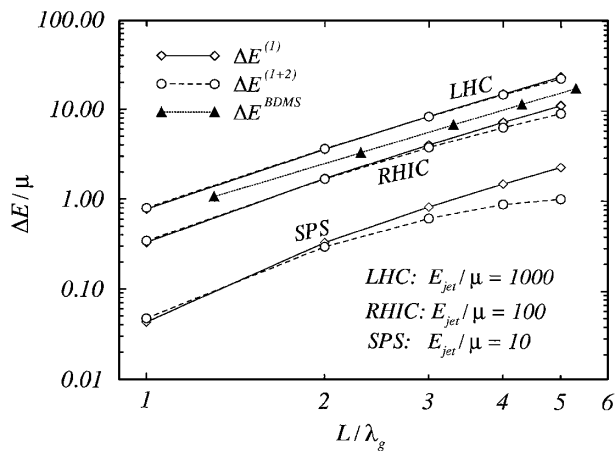
FIG. 3.   The radiated energy loss of a quark jet with energy E_{jet} = 5, 50, 500 GeV (at SPS, RHIC, LHC) is plotted as a function of the opacity L/λ_g. (λ_g = 1 fm, μ = 0.5 GeV.) Solid curves show first order, while dashed curves show results up to second order in opacity. The energy loss (solid triangles) from Refs. [3,7] (with $\tilde{\nu}$ = 2.5) is shown for comparison.

by 10%–30%, e.g., $N(\infty) = 8/3$ vs 4. Together with the logarithmic dependence on energy, these kinematic effects suppress greatly the energy loss at lower (SPS) energies as seen in Fig. 3. This is in contrast to the approximately energy independent result in Ref. [6] where the finite kinematic bounds were neglected. We note that the result of [6–8] should not be compared to the lower (SPS) energy since the $E > E_{cr} = L^2\mu^2/\lambda$ condition is violated at $L > 2$ fm for 5 GeV jets.

Conclusions.—We calculated the effect of final state interactions on the induced gluon differential distribution up to second order in opacity for hard jets produced in nuclear reactions. This work generalizes Ref. [5] by taking into account virtual corrections to calculate inclusive rates and provides a complementary analytic approach to clarify nonlinear jet quenching effects predicted in Refs. [3,6–8]. The inclusive $x dN/dx d\mathbf{k}_\perp^2$, dI/dx, and ΔE, were studied as a function of nuclear thickness for jet energies in the SPS, RHIC, and LHC range. One of our main results is the demonstration that the second order contribution (11) to the integrated energy loss remains surprisingly small up to realistic nuclear opacities $L/\lambda_g \sim 5$ (except at low SPS energies). The rapid convergence of the opacity expansion even for realistic opacities results from the fact that the effective expansion parameter is actually the product of the opacity and the gluon formation probability $L\mu^2/2xE$ [see (14)]. The leading quadratic dependence of the energy loss on nuclear thickness therefore arises from the simple first order term (7) in this approach. The detailed pattern of angular broadening and the x dependence is also dominated by the first order contribution. We note that our first order (effectively power-law) $|\mathbf{k}_\perp|$ and x distributions, however, differ considerably from the Gaussian form obtained in the eikonal resummation approach of [3,6] that applies to thick

targets. Surprisingly, on the other hand, the magnitude of the integrated $\Delta E(L)$ is rather similar at RHIC energies.

At SPS energies kinematic effects suppress greatly the energy loss relative to [6]. Our estimates provide a natural explanation for the absence of jet quenching in Pb + Pb at 160 AGeV that has been a puzzle up to now [10,11]. The short duration of the dense phase further limits the effective opacity at the SPS. A duration of $L/\lambda_g \sim 2$, for example, leads to a total energy loss of only ~ 100 MeV, which is much too small to be observable in soft multiple scattering background [11]. At RHIC energies, on the other hand, a significant nonlinear (in A) pattern of suppression [1,2] of high $p_\perp$ hadrons relative to scaled pp data should be observable to enable a direct test of non-Abelian energy loss mechanisms in dense matter. We note finally that the simplicity of the first and second order results (7),(11) will make it possible to improve significantly Monte Carlo event simulations of jet quenching [2].

Note added.—An independent opacity expansion also recently appeared in [14]. We have checked that up to second order our results coincide for the box geometry assumed there. Unlike the implicit integral relations derived in [14], our algebraic (reaction operator) derivation in [12] leads to compact analytic expressions for $P^{(n)}$.

[1] M. Gyulassy and M. Plümer, Phys. Lett. B **243**, 432 (1990); M. Gyulassy, M. Plümer, M. H. Thoma, and X.-N. Wang, Nucl. Phys. A **538**, 37c (1992).

[2] X.-N. Wang and M. Gyulassy, Phys. Rev. Lett. **68**, 1480 (1992).

[3] R. Baier, Yu. L. Dokshitzer, A. H. Mueller, and D. Schiff, Phys. Rev. C **60**, 064902 (1999).

[4] M. Gyulassy and X.-N. Wang, Nucl. Phys. **B420**, 583 (1994).

[5] M. Gyulassy, P. Lévai, and I. Vitev, Nucl. Phys. **B571**, 197 (2000); Nucl. Phys. **A661**, 637c (1999).

[6] R. Baier, Yu. L. Dokshitzer, A. H. Mueller, S. Peigné, and D. Schiff, Nucl. Phys. **B483**, 291 (1997); **484**, 265 (1997).

[7] R. Baier, Yu. L. Dokshitzer, A. H. Mueller, and D. Schiff, Nucl. Phys. **B531**, 403 (1998).

[8] B. G. Zhakharov, JETP Lett. **63**, 952 (1996); **65**, 615 (1997).

[9] U. A. Wiedemann and M. Gyulassy, Nucl. Phys. **B560**, 345 (1999).

[10] X.-N. Wang, Phys. Rev. Lett. **81**, 2655 (1998).

[11] M. Gyulassy and P. Levai, Phys. Lett. B **442**, 1 (1998).

[12] M. Gyulassy, P. Levai, and I. Vitev, Nucl. Phys. **B594**, 371 (2000).

[13] U. A. Wiedemann, Nucl. Phys. **B582**, 409 (2000).

[14] U. A. Wiedemann, Nucl. Phys. **B588**, 303 (2000).